VIP Catalytic Oxidation

DOI: 10.1002/anie.200605170

Metalloenzyme-Inspired Catalysis: Selective Oxidation of Primary Alcohols with an Iridium–Aminyl-Radical Complex**

*Martin Königsmann, Nicola Donati, Daniel Stein, Hartmut Schönberg, Jeffrey Harmer, Anandaram Sreekanth, and Hansjörg Grützmacher**

Complexes of redox-active metals and oxygen-centered radicals (tyrosinyl (TyrO$^{\bullet}$), O$^{\bullet-}$, or $O_2^{\bullet-}$) have highly specific functions in biological systems.[1–5] The copper-dependent metalloenzyme galactose oxidase (GOase)[6] specifically dehydrogenates (oxidizes) primary alcohols to the corresponding aldehydes at very high turn over frequencies (TOF) of greater than $2.5\times10^6\ h^{-1}$. The simplified catalytic cycle shown in Scheme 1 highlights the roles of the Cu^{2+} center and the coordinated TyrO$^{\bullet}$ radical in this process. The catalytic cycle starts with the coordination of the alcohol substrate R-CH_2OH to the Cu^{2+} center, in proximity to the TyrO$^{\bullet}$ radical (Scheme 1 a). The transfer of an α-hydrogen atom from the alcohol to the TyrO$^{\bullet}$ radical via the transition state **TS** (b) leads to a coordinated ketyl radical R-HC$^{\bullet}$-O (c), which is intramolecularly oxidized by the Cu^{2+} center to give the aldehyde R-CH=O (d). The resulting copper(I)–tyrosine complex is subsequently oxidized by molecular O_2, thereby turning over the catalytic cycle (e).

The catalytic reaction corresponds to a transfer hydrogenation, R-CH_2OH + O=X → R-CH=O + HO-XH, in which an O_2 molecule (X = O) acts as the H_2 acceptor. Transfer hydrogenations using ketones (X = CR_2) as the H_2 scavengers are catalyzed with high efficiency by diamagnetic organometallic complexes. The proposed mechanisms do not involve redox reactions.[7] Numerous copper complexes[8–13] and a wide range of other transition-metal complexes catalyze the oxidation of alcohols to carbonyl compounds, and some of these may even be used in combination with O_2 or H_2O_2 as the primary oxidants.[14] However, improvements of the activity and chemoselectivity remain desirable.[15] Herein, we report that iridium–aminyl-radical complexes catalyze the dehydrogenation of alcohols to aldehydes, with 1,4-benzoquinone (**BQ**) as the H_2 acceptor; primary non-activated alcohols, in particular, can be converted with very high activity and selectivity.

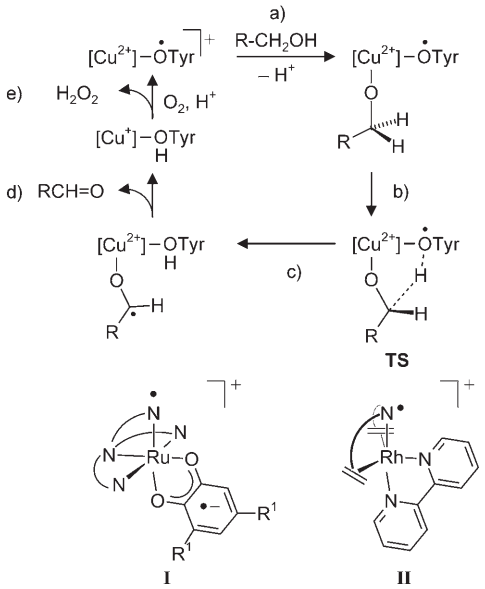

Scheme 1. Top: Simplified catalytic cycle for the GOase-catalyzed dehydrogenation of primary alcohols, highlighting the roles of the Cu^{2+} center and the coordinated TyrO$^{\bullet}$ radical. Bottom: Aminyl-radical complexes **I** (with bis(2-pyridylmethyl)-2-aminoethylamine as ligand and R^1 = *t*Bu) and **II** (with trop$_2$NH as ligand; see Scheme 2 for the formula of trop).

Calculations predict that complexes of late transition metals with the TyrO$^{\bullet}$ radical may be efficient models for GOase.[16] Recently, Tanaka et al. proposed the ruthenium(II)–aminyl-radical complex **I** (Scheme 1) as a key intermediate in the electrocatalytic dehydrogenation of alcohols to aldehydes.[17] We reported that rhodium–aminyl-radical complexes such as **II** (Scheme 1), in which approximately 60% of the spin population of the unpaired electron is located on the aminyl nitrogen atom,[18,19] are capable of abstracting hydrogen atoms from a variety of substrates.

The iridium complex that we use in the catalytic dehydrogenation of alcohols can be synthesized in two simple steps (Scheme 2): 1) the reaction of the tetradentate ligand trop$_2$dach[20] (**1**) with [Ir$_2$(μ-Cl)$_2$(coe)$_4$] (trop$_2$dach = *N*,*N*-bis(5-*H*-dibenzo[*a*,*d*]cycloheptene-5-yl)-1,2-diaminocyclohexane, coe = cyclooctene) in the presence of AgOTf ($OTf^- = CF_3SO_3^-$) to give orange-red [Ir(trop$_2$dach)]OTf (**2**); 2) the deprotonation of this remarkably acidic complex ($pK_a^{1(dmso)} = 10.5$, $pK_a^{2(dmso)} = 19.6$) with KO*t*Bu in THF or chlorobenzene to give first the red neutral amino amido complex [Ir(trop$_2$dach–H)] (**3**) and then the deep burgundy

[*] Dr. M. Königsmann, Dr. N. Donati, Dr. D. Stein, Dr. H. Schönberg, Prof. Dr. H. Grützmacher
Laboratory of Inorganic Chemistry
Department of Chemistry and Applied Biosciences
ETH Zürich, 8093 Zürich (Switzerland)
Fax: (+41) 446-331-418
E-mail: gruetzmacher@inorg.chem.ethz.ch
Dr. J. Harmer, Dr. A. Sreekanth
Laboratory of Physical Chemistry
Department of Chemistry and Applied Biosciences
ETH Zürich, 8093 Zürich (Switzerland)
E-mail: harmer@phys.chem.ethz.ch

[**] This work was supported by the Swiss National Science Foundation and the ETH Zürich.

Supporting information for this article is available on the WWW under http://www.angewandte.org or from the author.

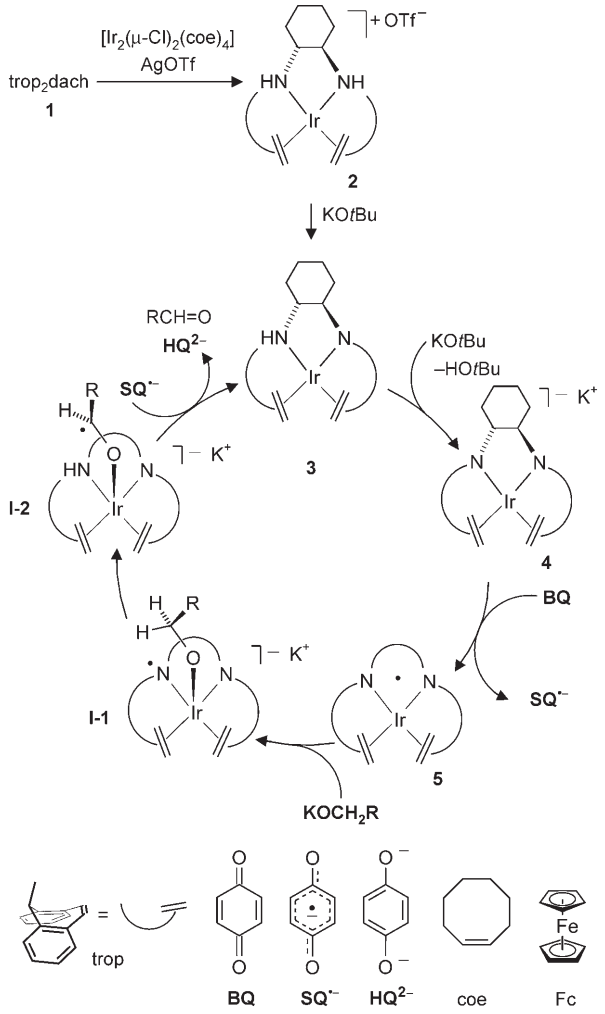

Scheme 2. Preparation of **4** and proposed catalytic cycle for the dehydrogenation of primary alcohols. **BQ** or Fc^+ can be used as the oxidant.

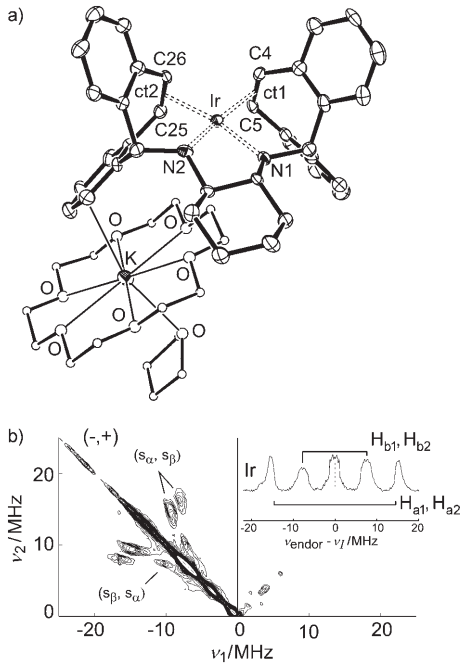

Figure 1. a) Structure of (*R*,*R*)-[K(thf)([18]crown-6)][Ir(trop$_2$dach−2H)]. Only one of the two crystallographically independent molecules is shown. The cation is represented as a ball-and-stick model. The hydrogen atoms and two THF molecules in the crystal lattice are omitted for clarity. Selected bond lengths [Å] and angles [°]: Molecule 1: Ir–N1 1.988(3), Ir–N2 1.961(3), Ir–ct1 1.996(4), Ir–ct2 2.002(4), C4–C5 1.445(6), C25–C26 1.444(6); sum of angles at N1: 348.9, sum of angles at N2: 356.4, dihedral angle between the N1-Ir-ct1 and N2-Ir-ct2 planes: 6.0. Molecule 2: IrA–N1A 1.970(3), IrA–N2A 1.962(3), IrA–ct1A 1.995(4), IrA–ct2A 2.001(4), C4A–C5A 1.440(6), C25A–C26A 1.442(6); sum of angles at N1A: 352.4, sum of angles at N2A: 353.2, dihedral angle between the N1A-IrA-ct1A and N2A-IrA-ct2A planes: 10.3. b) The Q-band HYSCORE spectrum (35.3 GHz) of **5** measured at 20 K at the echo maximum of the field-swept EPR spectrum. The cross peaks are assigned to single quantum transitions from the α and β electron spin manifolds of the nitrogen atoms N1 and N2. Inset: Proton region of the Davies ENDOR spectrum of **5**. The two sets of peaks centered about the proton Larmor frequency ν_I are assigned to two pairs of protons, H_{a1}/H_{a2} and H_{b1}/H_{b2}. The peak at ν_I originates from many protons in the vicinity of the unpaired electron.

anionic diamido complex [Ir(trop$_2$dach−2H)]$^-$ (**4**; trop$_2$dach−H and trop$_2$dach−2H denote the singly and doubly deprotonated forms of the ligand).

Complex **4** was characterized as the crown-ether adduct (*R*,*R*)-[K(thf)([18]crown-6)][Ir(trop$_2$dach−2H)] by single-crystal X-ray diffraction (Figure 1a).[21] The rigidity and steric encumbrance imposed by the trop$_2$dach ligand are clearly evident. The structure closely resembles those of analogous rhodium complexes.[19,22] Notably, the [K(thf)([18]crown-6)]$^+$ ion has a contact (3.3 Å) to one of the benzo groups of the [Ir(trop$_2$dach−2H)]$^-$ complex, and the coordination geometries of the two nitrogen centers are slightly pyramidal (Figure 1a).

Adding an oxidant (ferrocenium (Fc^+) or **BQ**) to a THF or chlorobenzene solution of **4** gives the transient radical **5** and the semiquinone radical anion (**SQ**$^{\bullet-}$; Scheme 2), which was unambiguously identified by its five-line electron paramagnetic resonance (EPR) spectrum.[23] The radical **5** is rather unstable, and attempts to isolate it always resulted in the formation of the amino amido complex **3**. Upon oxidation of **4** with FcOTf, **5** can be detected by pulse EPR spectroscopy, which gives some insight into its electronic structure. Hyperfine sublevel correlation (HYSCORE) and electron–nuclear double resonance (ENDOR) spectra (Figure 1b) show signals from two strongly coupled nitrogen nuclei (N1 and N2 with hyperfine coupling constants of $A = (-2, -2, 37)$ MHz) and four protons (H_{a1} and H_{a2} with $A = (29, 31, 38)$ MHz, and H_{b1} and H_{b2} with $A = (14, 15, 20)$ MHz; see the Supporting Information).[24]

The electronic structure of **5** is very similar to that of the analogous rhodium complex, which we proposed to be essentially equivalent to that of **4** after a one-electron oxidation.[19] However, as the fit between the experimental EPR spectroscopic parameters and those calculated by density functional theory (DFT) for a model analogous to that proposed for the rhodium complex is rather poor, we refrain from making a definite assignment of the electronic structure of **5**. We expect that the proton couplings originate

from either the benzyl protons of the trop residue and/or the β and γ protons of the cyclohexane ring. The small shift of the *g* values in the EPR spectrum of **5** ($g_1 = 1.974$, $g_2 = 1.993$, $g_3 = 2.028$) relative to that of the free electron ($g_e = 2.0023$) indicates that the unpaired electron is predominantly delocalized over the organic ligand and is not localized at the metal center (see the Supporting Information).

In the presence of the diamido complex **4** and with O_2 as the H_2 acceptor, benzyl alcohol is quantitatively converted to benzaldehyde in a stoichiometric reaction. The metal-containing product of this reaction is probably an iridium(III)–hydroxide complex, from which **4** cannot be regenerated. However, if the storable, stable precursor **2** and the H_2 acceptor **BQ** are used, a highly active and selective catalyst system is obtained for the dehydrogenation (oxidation) of primary alcohols to the corresponding aldehydes (Table 1).[25] With only 0.01 mol% of **2** and 0.01–0.1 mol% of KO*t*Bu, in chlorobenzene at 80–100°C, benzyl alcohol is nearly completely converted to benzaldehyde in 3 min; the corresponding TOF is greater than 150000 h^{-1} (entry 1). Quantitative conversions are also achieved at room temperature, although with lower catalyst activity (entries 2, 4, 9). Methylthioether (entry 3) or heterocyclic substrates (entries 4, 8, 9) are converted in good to excellent yields, and allylic alcohols are also smoothly converted (data not reported herein). Non-activated aliphatic alcohols such as methanol, ethanol, and particularly octanol are very rapidly dehydrogenated to the corresponding aldehydes (entries 5–7). Most remarkably, the highly selective dehydrogenation of 1,3-butanediol gives 3-hydroxybutanal exclusively. To our knowledge, no other transition-metal complex or GOase model system show comparable activity and chemoselectivity. In the dehydrogenation of the dihydroxy compounds 1,4-pentanediol (entry 11) and 1,2-di(hydroxymethylene)cyclohexane (entry 12) with 2 equiv **BQ**, the corresponding lactones are obtained in excellent yields at TOFs greater than 60000 h^{-1}. We assume that, in these reactions, the primary alcohol function is also selectively converted: an intramolecular cyclization to a semiacetal is followed by a rapid noncatalytic dehydrogenation by **BQ**. The hydroquinone (**HQ**) produced in the reaction precipitates and can be nearly quantitatively re-oxidized to the H_2 acceptor **BQ**.[25,26]

We propose the catalytic cycle shown in Scheme 2, which is supported by the following observations: 1) A mixture of **BQ**, $\mathbf{SQ}^{\bullet-}$, and $\mathbf{HQ}^{2-}$ alone does not lead to dehydrogenation. 2) No reaction is observed in the absence of the base KO*t*Bu. However, 1 equiv KO*t*Bu with respect to **2** is sufficient to start the catalysis; with 2 equiv KO*t*Bu, excellent results are obtained. 3) The formation of the deep violet $\mathbf{SQ}^{\bullet-}$ radical anion is detected in all the reactions. 4) In a dehydrogenation of benzyl alcohol, the amino amido complex **3** was recovered in addition to benzaldehyde at the end of the reaction.

Ambiguity remains with respect to the intermediates **I-1** and **I-2** (Scheme 2), for which we have no experimental evidence. When the substrate coordinates to the iridium center in close proximity to the aminyl nitrogen atom in **I-1**, the ketyl-radical complex **I-2** could be generated through an intramolecular hydrogen-atom transfer reaction. This step is the rate-limiting step in GOase-catalyzed reactions (isotope effect: $k_H/k_D \approx 22$). When the deuterated substrate C_6D_5-CD_2OH is used in catalytic runs with $[Ir(trop_2dach{-}2H)]^-$, we find a much smaller isotope effect ($k_H/k_D \approx 2$). We assume that the coordinated ketyl radical in **I-2** is intermolecularly oxidized by $\mathbf{SQ}^{\bullet-}$,[27] while in the GOase-catalyzed reactions with Cu^{2+} as the oxidant, this step proceeds intramolecularly (Scheme 1d).

Although we do not know the exact structure nor the fate of the radical **5** under the catalytic conditions, the EPR

Table 1: Catalytic dehydrogenation of alcohols to aldehydes.[a]

Entry	Substrate	Product[b]	Yield [%]	*t*	Entry	Substrate	Product[b]	Yield [%]	*t*
1	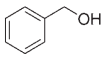	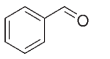	94	3 min	7	$C_7H_{15}CH_2OH$	$C_7H_{15}CH{=}O$	>98	10 min
2	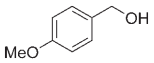	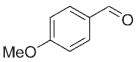	>98	16 h[c]	8			>98	12 h
3	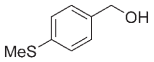	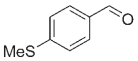	70	1 h	9			>98	2 h[c]
4	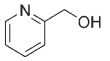	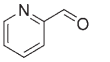	>98	3 h[c]	10	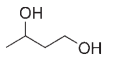	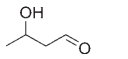	>98	1 h
5	CH_3OH	$CH_2{=}O$	64	4 h	11	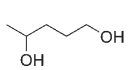		>98	10 min[d]
6	$MeCH_2OH$	$MeCH{=}O$	94	4 h	12	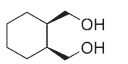		>98	5 min

[a] With **BQ** as the H_2 scavenger, 0.01 mol% **2**, and 0.03 mol% KO*t*Bu in chlorobenzene at 80°C. [b] The identity of each product was verified by gas GC, MS, and ^1H NMR spectroscopy through comparison with a reference sample. [c] In chlorobenzene at 25°C. [d] In chlorobenzene/THF (3:1) at 100°C.

spectroscopic data indicate that an iridium–nitrogen-radical complex plays an important role in the catalytic transfer dehydrogenation of the alcohols. The efficiency of this reaction is comparable to that of the transfer hydrogenation of carbonyl compounds promoted by diamagnetic transition-metal complexes. The reactions reported herein complement this chemistry and should be of equally high synthetic value.

Experimental Section

2: $[Ir_2(\mu_2\text{-}Cl)_2(coe)_4]$ (300 mg, 0.34 mmol) was dissolved in THF (25 mL), and $trop_2dach$ (**1**; 331 mg, 0.68 mmol) and a few drops of CH_3CN were added. Subsequently, AgOTf (172 mg, 0.68 mmol) was added to this mixture. After stirring for 1 h at room temperature, the mixture was filtered and concentrated in vacuo. Red crystals were grown from THF/hexane (1:1). Yield: 259 mg (309 mmol, 91 %). M.p. (decomp.): 208–212 °C. ^{1}H NMR (300.1 MHz, [D$_8$]THF): $\delta = 4.02$ (d, $^3J_{H,H} = 12.0$ Hz, 2H, CH^{olefin}), 4.75 (d, $^3J_{H,H} = 11.7$ Hz, 2H, CH^{olefin}), 5.53 (s, 2H, CH^{benzyl}), 5.92 (s br, 2H, NH), 7.41–7.72 ppm (m, 16H, CH^{ar}). ^{13}C NMR (62.9 MHz, [D$_8$]THF): $\delta = 53.0$ (s, 2C, CH^{benzyl}), 60.4 (s, 2C, CH^{olefin}), 67.5 ppm (s, 2C, CH^{olefin}). UV/Vis (THF): $\lambda_{max} =$ 486 nm.

3: The addition of 1 equiv KO*t*Bu to **2** in [D$_8$]THF led to a deep red solution of the neutral amino amido complex **3**, which was characterized by NMR spectroscopy. ^{1}H NMR (300.1 MHz): signals for four inequivalent olefinic protons: $\delta = 2.66$ (d, $^3J_{H,H} = 8.5$ Hz), 3.34 (d, $^3J_{H,H} = 8.3$ Hz), 3.46 (d, $^3J_{H,H} = 8.5$ Hz), 4.09 ppm (d, $^3J_{H,H} =$ 8.5 Hz); signal for NH: $\delta = 5.74$ ppm (d, $^3J_{H,H} = 12.5$ Hz). ^{13}C NMR (62.9 MHz): signals for four inequivalent olefinic carbon nuclei: $\delta =$ 47.8, 51.4, 54.8, 62.9 ppm. UV/Vis (THF): $\lambda_{max} = 504$ nm.

4: To a solution of **2** (100 mg, 0.12 mmol) in THF, KO*t*Bu (29 mg, 0.26 mmol) and [18]crown-6 (32 mg, 0.12 mmol) were added. The color of the reaction mixture changed to dark red. After layering the mixture with *n*-hexane, red crystals of **4** grew overnight. Yield: 101 mg (0.11 mmol, 94 %). M.p. (decomp.): 186–189 °C. ^{1}H NMR (300.1 MHz, [D$_8$]THF): $\delta = 2.63$ (d, $^3J_{H,H} = 8.3$ Hz, 2H, CH^{olefin}), 2.91 (d, $^3J_{H,H} = 8.5$ Hz, 2H, CH^{olefin}), 5.32 ppm (s, 2H, CH^{benzyl}). ^{13}C NMR (62.9 MHz, [D$_8$]THF): $\delta = 49.8$ (s, 2C, CH^{olefin}), 52.5 (s, 2C, CH^{olefin}), 65.8 ppm (s, 2C, CH^{benzyl}). UV/Vis (THF): $\lambda_{max} = 524$ nm.

Catalyses: The catalyst precursor **2** (6 μmol) was dissolved in chlorobenzene (25 mL) at the temperature given in Table 1. Subsequently, KO*t*Bu (6–18 μmol) was added, and after 5 min stirring, the substrate (60 mmol) was added. After another 5 min, freshly sublimed **BQ** (8.6 g, 80 mmol) was added to the reaction mixture. The progress of the reaction was monitored by GC and ^{1}H NMR spectroscopy. Further details are given in the Supporting Information.

Received: December 21, 2006
Published online: March 30, 2007

Keywords: alcohols · homogeneous catalysis · iridium · oxidation · radicals

[1] M. Fontecave, J.-L. Pierre, *C. R. Acad. Sci. Ser. IIc* **2001**, *4*, 531.
[2] M. Fontecave, J.-L. Pierre, *Bull. Soc. Chim. Fr.* **1996**, *133*, 653.
[3] J. Stubbe, W. A. van der Donk, *Chem. Rev.* **1998**, *98*, 705.
[4] F. Himo, P. E. M. Siegbahn, *Chem. Rev.* **2003**, *103*, 2421.
[5] P. R. Ortiz de Montellano, *Cytochrome P450: Structure, Mechanism, and Biochemistry*, 3rd ed., Kluwer, New York, **2005**.
[6] J. W. Whittaker, *Arch. Biochem. Biophys.* **2005**, *433*, 227.
[7] a) J. S. M. Samec, J.-E. Bäckvall, P. G. Andersson, P. Brandt, *Chem. Soc. Rev.* **2006**, *35*, 237; b) S. Gladiali, E. Alberico, *Chem. Soc. Rev.* **2006**, *35*, 226.
[8] P. Chaudhuri, K. Wieghardt, T. Weyhermüller, T. K. Paine, S. Mukherjee, C. Mukherjee, *Biol. Chem.* **2005**, *386*, 1023.
[9] J.-L. Pierre, F. Thomas, *C. R. Chim.* **2005**, *8*, 65.
[10] R. C. Pratt, T. D. P. Stack, *Inorg. Chem.* **2005**, *44*, 2367.
[11] P. Gamez, I. A. Koval, J. Reedijk, *Dalton Trans.* **2004**, 4079.
[12] B. A. Jazdewski, W. B. Tolman, *Coord. Chem. Rev.* **2000**, *200–202*, 633.
[13] I. E. Markó, P. R. Giles, M. Tsukazaki, S. M. Brown, C. J. Urch, *Science* **1996**, *274*, 2044.
[14] Reviews: a) S. V. Ley, J. Norman, W. P. Griffith, S. P. Marsden, *Synthesis* **1994**, 639; b) R. A. Sheldon, I. W. C. E. Arends, A. Dijksman, *Catal. Today* **2000**, *57*, 157; c) R. A. Sheldon, I. W. C. E. Arends, G.-J. ten Brink, A. Dijksman, *Acc. Chem. Res.* **2002**, *35*, 774; d) R. Irie, T. Katsuki, *Chem. Rec.* **2004**, *4*, 96; e) S. S. Stahl, *Angew. Chem.* **2004**, *116*, 3480; *Angew. Chem. Int. Ed.* **2004**, *43*, 3400.
[15] The most active homogeneous catalyst in an Oppenauer oxidation yet described is $[IrCp^*(NHC)(MeCN)_2]^{2+}$ (Cp^* = pentamethylcyclopentadienyl; NHC = *N*-heterocyclic carbine), which reaches turnover numbers (TON) of approximately 7000: F. Hanasaka, K. Fujita, R. Yamaguchi, *Organometallics* **2005**, *24*, 3422.
[16] L. Guidoni, K. Spiegel, M. Zumstein, U. Röthlisberger, *Angew. Chem.* **2004**, *116*, 3348; *Angew. Chem. Int. Ed.* **2004**, *43*, 3286.
[17] Y. Mityazato, T. Wada, K. Tanaka, *Bull. Chem. Soc. Jpn.* **2006**, *79*, 745.
[18] T. Büttner, J. Geier, G. Frison, J. Harmer, C. Calle, A. Schweiger, H. Grützmacher, *Science* **2005**, *307*, 235.
[19] P. Maire, M. Königsmann, A. Sreekanth, J. Harmer, A. Schweiger, H. Grützmacher, *J. Am. Chem. Soc.* **2006**, *128*, 6578.
[20] P. Maire, F. Breher, H. Schönberg, H. Grützmacher, *Organometallics* **2005**, *24*, 3207.
[21] Crystal data for **4**: $C_{52}H_{64}IrKN_2O_7{\cdot}C_4H_8O$; crystal size: $0.31 \times 0.23 \times 0.21$ mm^3, monoclinic, space group $P2_1$, $a = 11.7856(7)$, $b =$ 24.750(1), $c = 17.254(1)$ Å, $\beta = 95.342(1)°$, $V = 5010.89$ Å^3, $Z = 4$, $\mu = 2.80$ mm^{-1}, $T = 200$ K, 69595 reflections, 24616 independent, $R_{int} = 0.0304$, 1225 parameters, 14 restraints, $R1 = 0.0302$ (for 22911 reflections with $I > 2\sigma(I)$), $wR2 = 0.0685$ (for all data), GooF = 1.032 (on F^2), max./min. residual electron density: 1.611/−0.502 e Å^{-3}. CCDC-622200 (**4**) contains the supplementary crystallographic data for this paper. These data can be obtained free of charge from The Cambridge Crystallographic Data Centre via www.ccdc.cam.ac.uk/data_request/cif.
[22] P. Maire, F. Breher, H. Grützmacher, *Angew. Chem.* **2005**, *117*, 6483; *Angew. Chem. Int. Ed.* **2005**, *44*, 6325.
[23] EPR (X-band, 298 K): $g = 2.005$, $a(^1H) = 6.7$ MHz. J. C. Chippendale, E. Warhurst, *J. Chem. Soc. Faraday Trans.* **1968**, *64*, 2332.
[24] A. Schweiger, G. Jeschke, *Principles of Pulse Electron Paramagnetic Resonance*, Oxford University Press, Oxford, **2001**.
[25] For the use of quinones as electron-transfer mediators in the ruthenium-catalyzed aerobic oxidation of secondary alcohols, see: G. Csjernyik, A. H. Éll, L. Fadini, B. Pugin, J.-E. Bäckvall, *J. Org. Chem.* **2002**, *67*, 1657.
[26] B. B. F. Mirjalili, M. A. Zolfigol, A. Bamoniri, A. Zarie, *Bull. Korean Chem. Soc.* **2003**, *24*, 400.
[27] Reduction potentials: PhCH=O/PhCH-O$^{\bullet-}$: −1.67 V; **BQ**/**SQ**$^{\bullet-}$: −0.54 V, **SQ**$^{\bullet-}$/**HQ**$^{2-}$: −1.4 V (vs. the saturated calomel electrode (SCE), aprotic solvents): a) V. P. Vanýsek in *CRC Handbook of Chemistry and Physics*, 87th ed., CRC, Boca Raton, **2006**, pp. 8–32; http://www.hbcpnetbase.com; b) A. J. Bard, L. R. Faulkner, *Electrochemical Methods*, Wiley, New York, **1980**, pp. 701–702.

